Establishing Traceability with a GPS Disciplined Clock: A Preliminary Report

ESTABLISHING TRACEABILITY WITH A GPS DISCIPLINED CLOCK: A PRELIMINARY REPORT

John W. Clark (1), Demetrios N. Matsakis (1), Andrew N. Novick (2), and Michael A. Lombardi (2)
(1) Masterclock, Inc., St. Charles, MO, 63301, Jclark@masterclock.com
(2) National Institute of Standards and Technology (NIST), Boulder, CO, 80305

ABSTRACT

The metrological definition of traceability requires a documented and unbroken chain of calibrations that each contribute to the measurement uncertainty [1]. The calibrations must be end-to-end, which for a Global Positioning System Disciplined Clock (GPSDC), must include the antenna and cabling. While understanding legal definitions may be arduous at times, working with metrology labs to develop detailed criteria can be constructive for GPSDC manufacturers. To establish the suitability of a GPSDC for traceability, we have compared the one pulse-per-second (PPS) outputs of several GPSDCs to the National Institute of Standards and Technology (NIST) realization of Coordinated Universal Time, termed UTC(NIST). The GPSDC measurements included the use of several different antennas, with results showing agreement to within to tens of nanoseconds of UTC(NIST). We will explain these measurements and provide estimations of their associated uncertainties.

INTRODUCTION

There are a variety of ways to calibrate a GPSDC system. An absolute calibration would require measurement of the timing difference between a known signal being input to the device and the PPS being output. The antenna can be separately calibrated, but it requires use of an anechoic chamber. The difficulty is compounded because time is indicated on the input GPS signal as the start-point of a code sequence that repeats every millisecond, whereas a new second is indicated on the output PPS when that pulse attains a specific voltage. Much simpler is a relative calibration, in which the rising edge of the output of a device under test (DUT) is calibrated against a previously-calibrated reference system using just the time difference between their PPS signals, as measured with a time interval counter (TIC). This paper describes such a relative calibration, where a national metrology institute (NMI)'s time scale is used to calibrate the DUT to agree with Coordinated Universal Time (UTC).

If the NMI hosts a receiver and antenna system that is fully calibrated, a relative calibration can be achieved by measuring the difference between the PPS signal of the NMI's GNSS system and the DUT, after accounting for the delays due to cables that are part of the test setup. An alternate way would be to measure the time difference between the NMI's realization of UTC, which is termed UTC(*k*). In this case, the basic formula to find the calibration delay value, or *CAL*, is

$$CAL = [\text{DUT} - \text{UTC}(k)] + [\text{UTC}(k) - \text{UTC(USNO)}] + [\text{UTC(USNO)} - \text{GPS Time}] ,$$

where the first bracketed term, DUT – UTC(*k*) is obtained via TIC measurements. The second bracketed term, UTC*(k)* – UTC(USNO), can be obtained from the Circular T, published monthly

by the International Bureau of Weights and Measures (BIPM) [2], or from the BIPM's weekly publication of Rapid UTC, known as UTCr [3]. UTC(NIST) – UTC(USNO), for example, is typically close to zero mean, with both a root mean square (RMS) and an uncertainty of about 3 ns. Since publication may not be released for several weeks after a measurement, we could choose to set UTC(NIST) – UTC(USNO) = 0 and increase the uncertainty's contribution to the error budget, with the option to revise it once the Circular T comes out. The third bracketed term UTC(USNO) – GPS Time is typically given at the annual meetings of the Civil GPS Interface Committee (CGSIC), available at gps.gov. It is 0 mean with an RMS of approximately 1 ns, so for all practical purposes it can be ignored. However the second and third bracketed terms are handled, we shall show that the largest contributor to the value and offset of *CAL* will likely be the measurement of DUT – UTC(*k*).

THE EXPERIMENTAL CONFIGURATIONS

The DUTs to be calibrated were several antenna/GPSDC combinations. The experimental arrangement included four GMR5000 GPS-disciplined clocks (manufactured by Masterclock, Inc.) and three different types of antennas, which we shall refer to as conical, magnetic, and disk. In essence, different antennas were fed into a signal splitter that delivered the same GPS signal to each of the four GMR5000s, and their outputs were compared to UTC(NIST) using separate TICs.

Figure 1. The conical antenna (left), the disk antenna (2nd), the magnetic antennas (3rd), and the GMR5000s with their TICs (right).

Figure 2 is a block diagram showing four GPSDCs along with the TICs used to measure their time differences with respect to UTC(NIST). The numbers in nanoseconds (ns) indicate the measured cable delays.

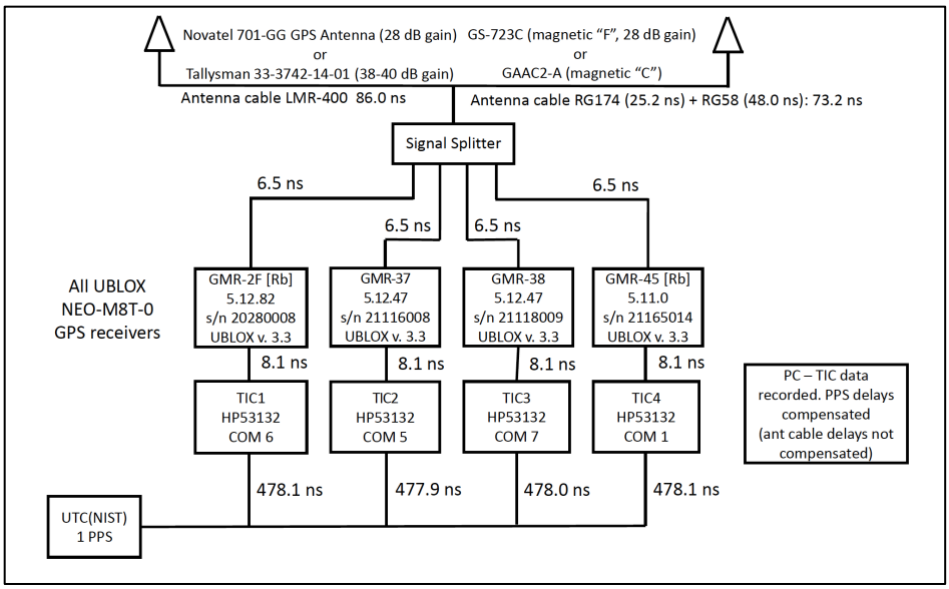

Figure 2. Block diagram of experimental setup.

In addition to the equipment shown, Common GNSS Generic Time Transfer Standard (CGGTTS) [4] formatted data from NIST's dual-frequency receiver reporting to the IGS (whose moniker is "NIST") and an uncalibrated single-frequency receiver (whose moniker is "GMNI"), both referenced to UTC(NIST) were used in a form of "Common View". To compare the CGGTTS formatted-data with a time series representing GPS – UTC(NIST), concurrent observations of each GPS satellite versus UTC(NIST) in the file were averaged for 13-minutes to match the CGGTTS format. In addition, the measured ionosphere correction in the dual-frequency CGGTTS data [5] was subtracted from the Klobuchar model [6] value, which is a model for the delay that utilizes parameters broadcast by the GPS satellites [7], and whose value is given in the single-frequency CGGTTS data for each satellite. Since the ionospheric data depends roughly as the sine of the elevation, the data for individual satellites were not averaged. However, a second set of data was created in which the difference between measured and modeled ionospheres were multiplied by the sine of the elevation angle.

To achieve the best timing results from a GPSDC, an accurate position must be known. Typically, GPSDCs determine both time and position simultaneously with a linear least squares fit using the GPS data but, because the receiver might be moving, they use only the most recent data. However, if it is stationary, more precise time could be obtained by fixing the spatial coordinates and only solving for the time. For this reason, many GPSDCs have a "survey mode", in which the position is fixed in a "hold mode" after some averaging time. The "survey mode" for the GPSDCs in this experiment only uses ten minutes of data averaging to determine the position, and they do not have the option to manually enter known coordinates. As the visible GPS constellation varies, there will be variations with a daily signature - it may not be sinusoidal but it could be composed of many-hour long sinusoidal arcs. Averaging the positioning data for 24 hours to attenuate any diurnal effects would produce a better result. For this experiment, most of the measurements were performed while the receivers were not in "survey mode".

MEASUREMENT RESULTS

Figure 3 displays all the data taken with the configuration described in the previous section. In this reduction, all the known effects of measuring components, namely the antenna splitter and the cables, have been removed. The vertical bars denote configuration changes.

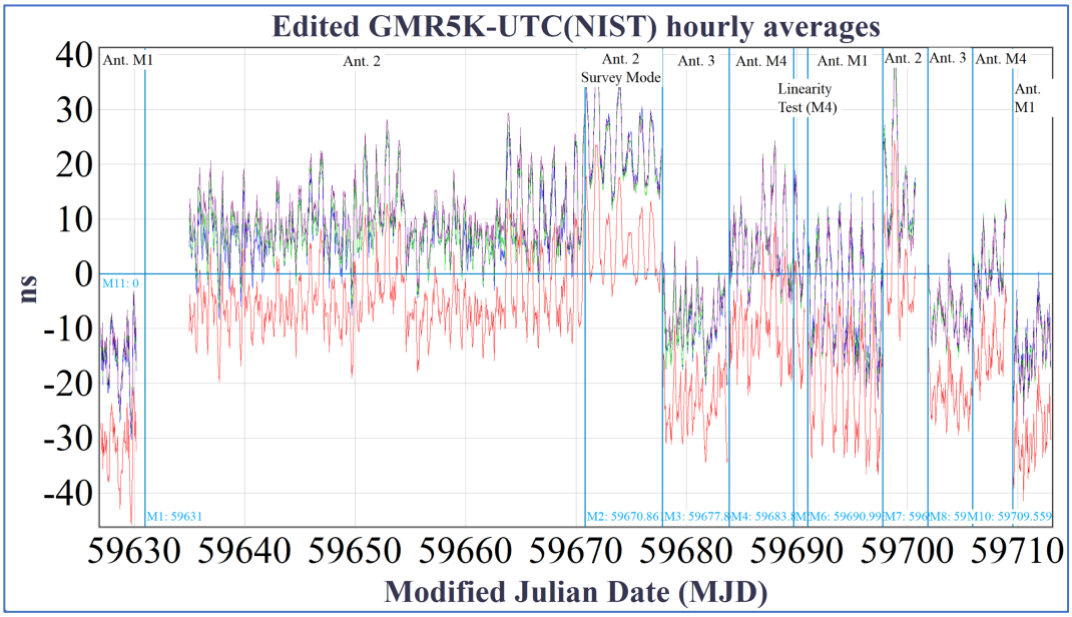

Figure 3. Approximately 100 days of GPSDC – UTC(NIST) data. A value of 0 implies that the GPSDC + antenna system is perfectly calibrated. Not shown are tests made to establish the linearity and inter-changeability of the cables, TICs, and splitter ports. Antennas with an "M" are magnetic, Antenna 2 is disk, and Antenna 3 is conical. Each GMR's curves have a unique color.

The most important thing to notice is that all of the GPSDCs, when averaged over a given configuration, are within 30 ns of zero calibration error. Changing the antenna can affect the results by up to 20 ns. Also, one of the GPSDCs consistently yields a time offset that differs from the others by -15 ns, but the other three GPSDCs are so similar that the plots largely fall on top of each other. The third configuration (labeled Ant. 2, survey mode) was identical to the second configuration except that the GPSDCs were set to survey mode, resulting in a large jump. Close inspection shows that there was a spike at the end of the previous series, which likely corresponds with an ionosphere fluctuation that impacted both position and timing; that position error remained at that point once survey mode was enabled. Another aspect of the data is that the repeatability of configurations was only at the 10 ns level (see for example the first and last configurations). We show below that this was due to a miscorrection of the single-frequency ionospheric Klobuchar model. We will also show that the several spikes in the data are due to the Klobuchar model failing to adequately represent the ionospheric delay.

Figure 4 shows the results when the GMR5000 – UTC(NIST) data were differenced with the data from the uncalibrated single-frequency receiver (GMNI), removing UTC(NIST) from the equation and showing only the "common view" difference between GMNI and the GMR5000s. We can see immediately that the repeat configurations are much closer to their initial values, to within ~3 ns. Had the receiver GMNI been calibrated, the figure would have been sufficient to calibrate the

DUTs. Since the DUTs have been calibrated as a result of the work shown in this paper, this plot can be used to establish the calibration of the GMNI.

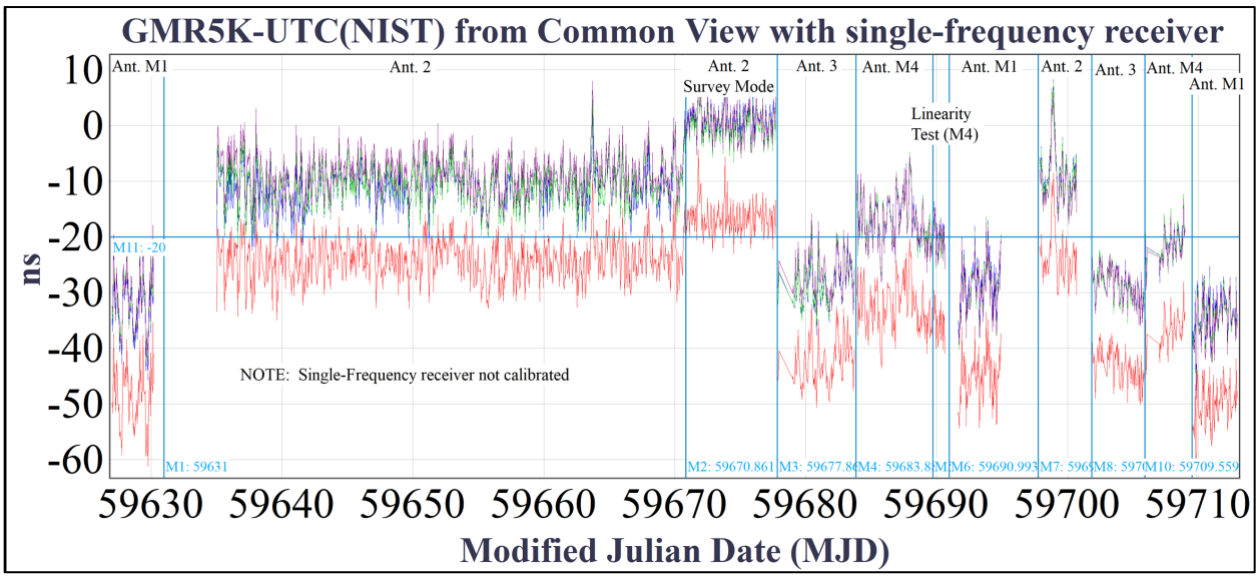

Figure 4. Common view-like difference between GMR5000s and the NIST single-frequency receiver known as GMNI. Plot annotations as in previous figure.

THE DATA ANALYSIS AND THE IONOSPHERE'S SIGNATURE

The improved repeatability shown in Figure 4 can be understood through the differences between the Klobuchar model and the measured ionosphere correction (Figure 5).

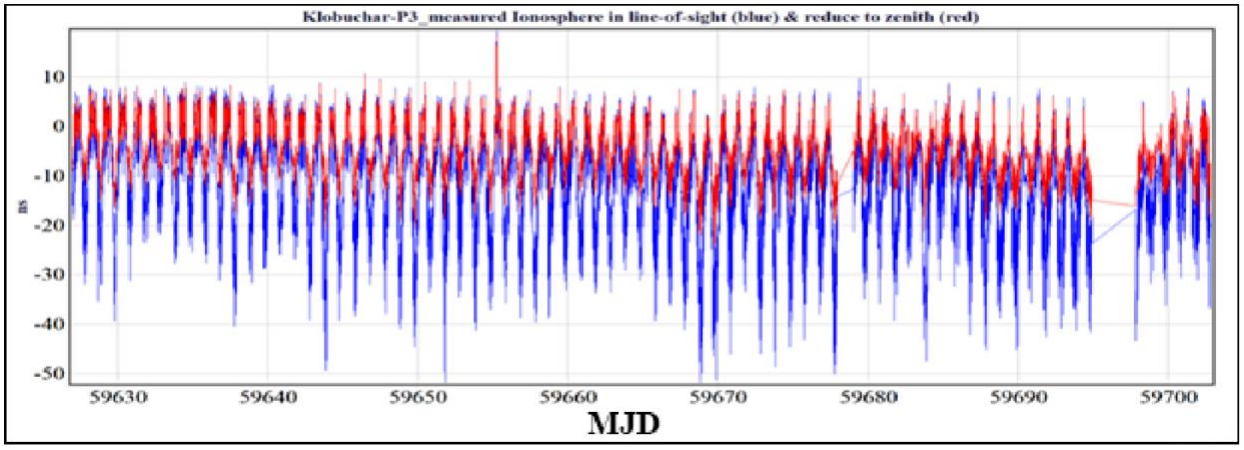

Figure 5. The satellite-averaged Klobuchar - Measured ionosphere corrections averaged over the line of sight (blue), and the difference when each satellite's data is multiplied by the sine of its elevation angle (red, inverted for clarity).

Figure 6 shows the daily averages of the two curves, without inverting the data multiplied by the sine of the elevation angle. The lower values towards the end are consistent with the drop seen in the GMR5000 – UTC(NIST) data of Figure 3.

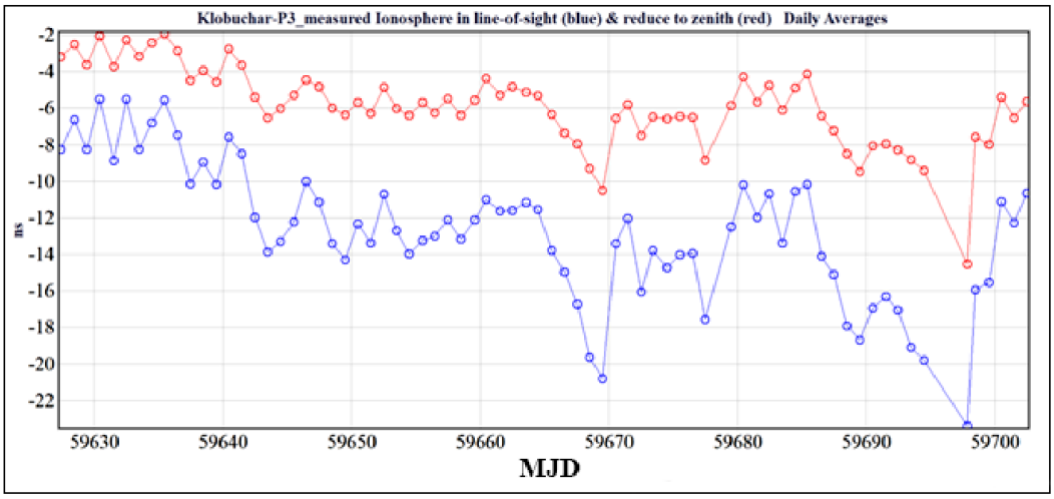

Figure 6. Daily averages of the ionosphere mismodeling data in the previous figure. The red curve is no longer inverted.

The mismodeled ionospheric effects can also be estimated by computing the actual time and position values a GMR5000 would find if its data were only the difference between the measured and modeled ionosphere. Figure 7 shows the time component of the solution, which is again consistent with the behavior observed in Figure 3.

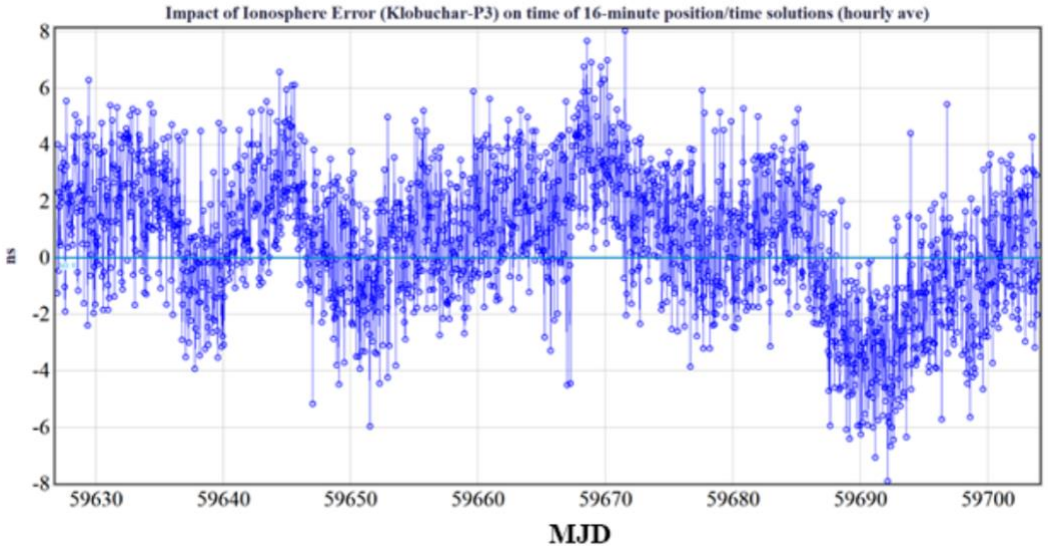

Figure 7. Time offsets that a GPSDC would infer from fits to GPS data, that would be due to mismodeling by the Klobuchar method.

The effects of external (outside) temperature, and perhaps humidity, on the antennas (which contain active elements) are probably minimal as inferred by observations. Figure 8 shows the data

from just one GPSDC superimposed upon a plot of the external temperature, and the difference between the modeled ionosphere and the measured ionosphere.

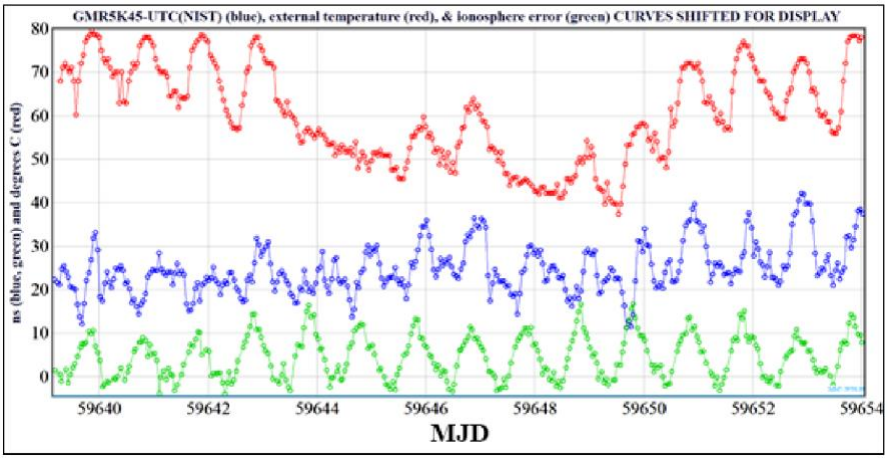

Figure 8. Fifteen days of data showing the diurnal signatures of a GMR5000 – UTC(NIST) (blue, middle), the external temperature (red, top), and the line-of-sight error in the Klobuchar ionospheric model (green).

Because the ionosphere peaks around solar noon, roughly seven hours before UTC midnight at Boulder, while the temperature peak is approximately about three hours later, it is not easy to separate their effects from the phase of the diurnals. However, the large temperature drop during the period from Modified Julian Date (MJD) 59643-59650 has no correlation with the PPS differences, and this supplements the evidence from Figure 4 about the ionosphere being the cause of the large variations seen in Figure 3.

To measure the effect of troposphere mismodeling, we can plot the measured satellite time offsets of the CGTTS data from the NIST and GMNI receivers as a function of elevation. The dual-frequency receiver would show the effect of the troposphere (Figure 9) as a slope, but there is no appreciable slope. The single-frequency receiver shows the combination of both troposphere and ionosphere (Figure 10), and there is slope of 0.09 ns/deg.

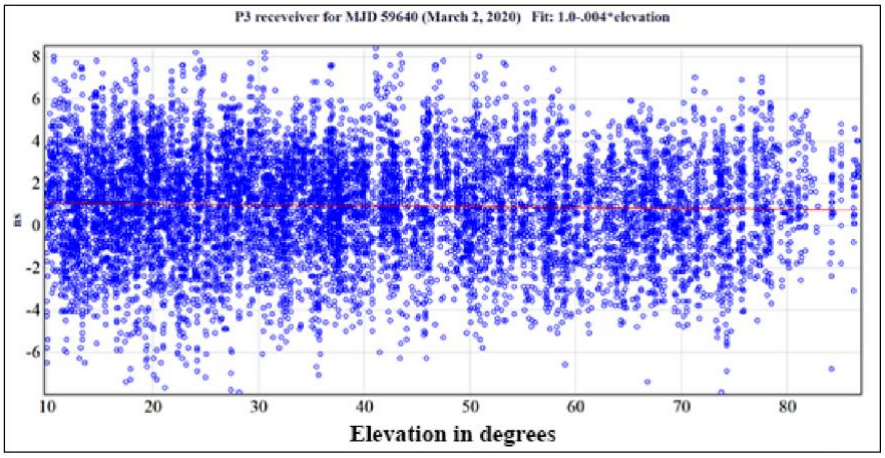

Figure 9. Time offset of GPS satellites vs. elevation as seen by dual-frequency receiver on MJD 59690. The barely visible red line is a least squares fit, fairly close to $y = 1$ ns.

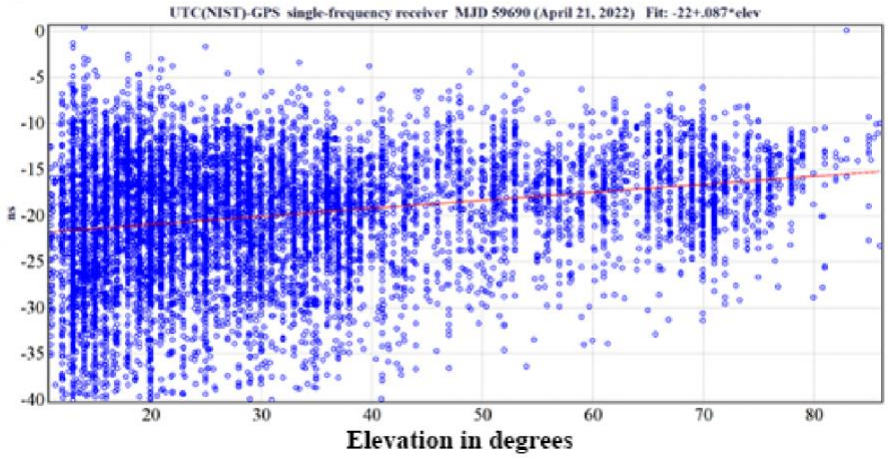

Figure 10. Time offset of GPS satellites vs. elevation angle as seen by dual-frequency receiver on MJD 59690. The red line is a linear fit.

A final consideration in our case is UTC(NIST) – UTC(USNO) were in very close agreement for the five-year period from April 2017 to April 2022, never differing by more than ±5 ns, as shown in Figure 11.

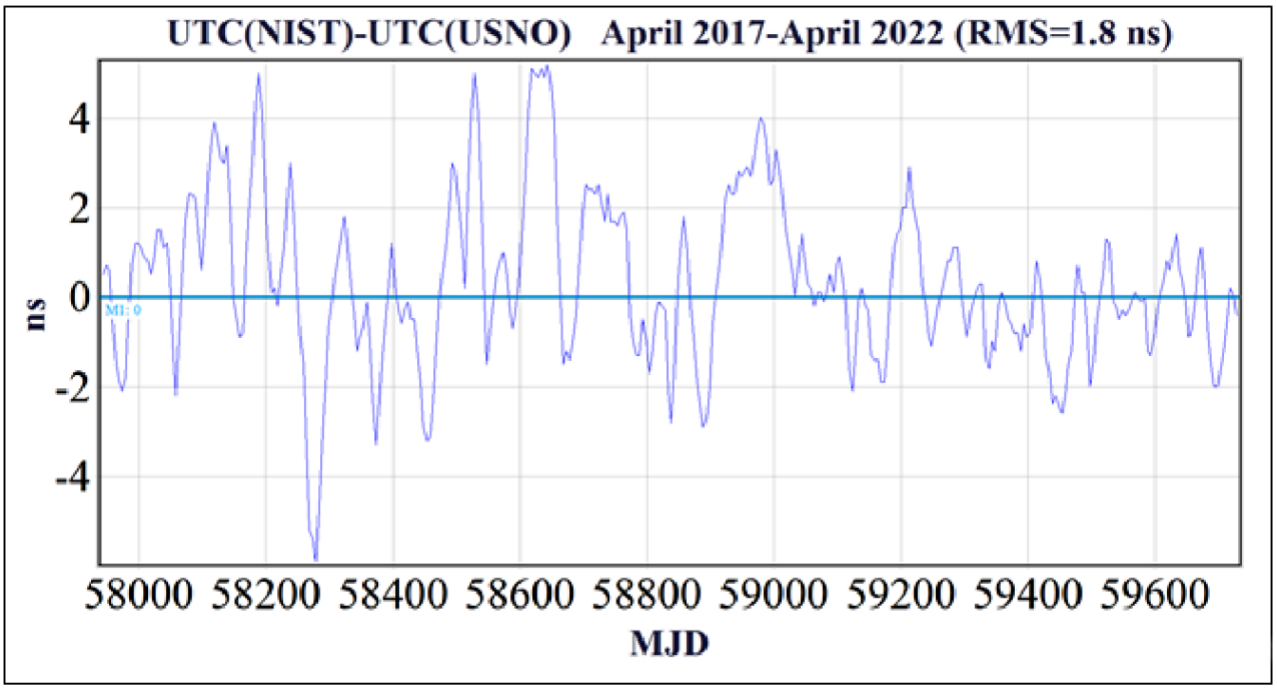

Figure 11. UTC(NIST) – UTC(USNO) from BIPM's Circular T.

CONCLUSION: MEASUREMENT UNCERTAINTY

Table 1 lists coarse estimates of the uncertainties as a result of this work. The last entry, GPS Time – UTC(USNO), would likely be reduced to < 1 ns if actual data from the USNO is available for

the period of calibration. Also, the uncertainty of UTC(NIST) – UTC(USNO) is the root sum of squares (RSS) of the combined total uncertainties for UTC – UTC(NIST) and UTC – UTC(USNO) as given in the Circular T. If we are not willing to wait for the Circular T, we must also include the RMS value of UTC(USNO) – UTC(NIST) in that RSS. Additionally, if we use UTCr instead of UTC, we must include a term in the RSS that corresponds to the RMS value of (UTC(NIST) – UTC(USNO) – UTCr(NIST) + UTCr(USNO)). For extended calibrations the Circular T statistical uncertainties (Type A) are reduced while the systematic uncertainties (Type B) are unchanged; the combined RMS is the RSS of the Type A and Type B uncertainties.

However, the uncertainty analysis shows that, for single-frequency receivers, all the above effects are dominated by the ionospheric effects, and so an uncertainty of 10 ns RMS, or 30 ns peak-to-peak is attained.

While these experiments are highly suggestive of a definite number, they were all taken while the DUTs were kept at a fairly constant laboratory temperature of 23 ^{O}C ± 1 ^{O}C. In future work, we shall quantify the temperature dependence of the DUTs, establish the constancy of the calibrations over time, and present more detailed numerical analysis.

ns*	Error Source
1	cabling
2	splitter
10	survey mode
< 30	sub-daily ionosphere (single frequency only)
< 10	multi-day ionosphere (single frequency only)
small	troposphere
small	temperature
3	UTC(NIST)-UTC(USNO) from BIPM's Circular T
1	GPS-UTC(USNO)
< 15	GPSDO relative factory cal
< 25	Antenna relative factor cal
< 30	Ionosphere limit
	* Upper limit are max deviations, otherwise RMS
	* Based only on the data observed in this talk

Table 1. Uncertainty Analysis for the GPSDC calibration.

DISCLAIMER

NIST, as a matter of policy, does not endorse any commercial products. Any references to such products are for the purpose of technical clarity. Other products may be found that work equally or better. J. Clark is CEO of Masterclock, Inc., which manufactured the GMR5000's used in this work, and Dr. Demetrios is the Chief Scientist.

ACKNOWLEDGEMENTS

We thank Lukas Burzynski and Robert Ottinger for a careful review of the manuscript, and EZL Software for the use of their data plotting and analysis package.

REFERENCES

[1] Joint Committee for Guides in Metrology (JCGM), "International Vocabulary of Metrology – Basic and General Concepts and Associated Terms," VIM, 3rd edition, *JCGM 200*, 2012.

[2] BIPM Time Department, "Circular T". Available monthly (from 1996 to present) at: https://www.bipm.org/en/time-ftp/circular-t

[3] BIPM Time Department, "UTCr". Available weekly (from 2013 to present) at: https://www.bipm.org/en/time-ftp/utcr

[4] P. Defraigne and G. Petit, "CGGTTS-Version 2E: and extended standard for GNSS Time Transfer," *Metrologia,* vol. 52, G1, 22 p., 2015.

[5] V. Zhang and Z. Li, "Measured ionospheric delay corrections for code-based GPS time transfer," *NCSLI Measure Journal of Measurement Science,* vol. 10, no. 3, pp. 66–71, September 2015.

[6] J. Klobuchar, "Ionospheric time-delay algorithm for single-frequency GPS users," *IEEE Transactions on Aerospace and Electronic Systems,* vol. AES-23, no. 3, pp. 325–331, 1987.

[7] Global Positioning Systems Directorate, "Navstar GPS Space Segment/Navigation User Interfaces," *Interface Specification IS-GPS-200H,* 2013.